UCRL-16905

University of California
Ernest O. Lawrence Radiation Laboratory

THE YIELD STRESS OF ALLOYS WITH COHERENT LAMELLAR MICROSTRUCTURES (I)

TWO-WEEK LOAN COPY

This is a Library Circulating Copy which may be borrowed for two weeks. For a personal retention copy, call Tech. Info. Division, Ext. 5545

Berkeley, California

DISCLAIMER

This document was prepared as an account of work sponsored by the United States Government. While this document is believed to contain correct information, neither the United States Government nor any agency thereof, nor the Regents of the University of California, nor any of their employees, makes any warranty, express or implied, or assumes any legal responsibility for the accuracy, completeness, or usefulness of any information, apparatus, product, or process disclosed, or represents that its use would not infringe privately owned rights. Reference herein to any specific commercial product, process, or service by its trade name, trademark, manufacturer, or otherwise, does not necessarily constitute or imply its endorsement, recommendation, or favoring by the United States Government or any agency thereof, or the Regents of the University of California. The views and opinions of authors expressed herein do not necessarily state or reflect those of the United States Government or any agency thereof or the Regents of the University of California.

UCRL-16905

Submitted to Acta Metallurgica

UNIVERSITY OF CALIFORNIA

Lawrence Radiation Laboratory
Berkeley, California

AEC Contract No. W-7405-eng-48

THE YIELD STRESS OF ALLOYS WITH COHERENT LAMELLAR MICROSTRUCTURES (I)

S. D. Dahlgren

May 1966

THE YIELD STRESS OF ALLOYS WITH COHERENT LAMELLAR MICROSTRUCTURES (I)

S. D. Dahlgren

Inorganic Materials Research Division, Lawrence Radiation Laboratory,
University of California, Berkeley, California

ABSTRACT

May 1966

The yield stress of alloys with lamellar microstructures is related to the internal coherency strains associated with individual lamellae. The results are as follows: (1) The yield stress is directly proportional to the difference in the cubic lattice parameters of the two chemically different lamellae forming the lamellar microstructure; (2) For alloys containing volume fractions of one kind of lamellae below the critical value of $\frac{1}{3}$, the yield stress is directly proportional to the volume fraction; (3) For alloys containing volume fractions between critical values ($\frac{1}{3}$ to $\frac{2}{3}$), the yield stress is independent of the volume fraction; (4) The yield stress is independent of the interlamellar spacing present.

first stage is called the "side-band" stage because of the satellite reflections which appear on either side of the main reflections in Debye-Sherrer x-ray patterns. These satellites are due to one-dimensional composition (and therefore lattice parameter) fluctuations in face-centered-cubic material. The satellite position with respect to the main Bragg line is a function of the wavelength of the composition fluctuation and is more removed from the main line the smaller the wavelength.[6] A sine wave[6] has been used to approximate the composition-distance curve although other investigators[7,8] have suggested that a square or more general wave shape would be just as appropriate. No method has been devised to ascertain experimentally the exact wave form that exists during the transformation.

The second stage x-ray patterns reveal the formation of two tetragonal structures.[4,7,9] The two non-equilibrium structures have a common "a" tetragonal lattice parameter which is constant throughout both structures. One of these structures has a c/a ratio less than one while the other has a c/a ratio greater than unity. The morphology of the two structures is lamellar with the plates lying parallel to {100} planes. The two tetragonal "a" axes lie in the common {100} plane and the "c" axes are normal to this plane.[4,6] It is apparent that the second stage structure also possesses a one-dimensional lattice parameter variation along the "c" axis which probably more nearly approaches a square wave configuration than is the case during the earlier "side band" stage. Because the fluctuation wavelength of the tetragonal state is larger than that of the "side-band" stage, the difference in stages one and two may be only one of degree. Bagaryatskii and Tyapkin[10,11] have shown for similar transformations found in Ni-Ti and Ni-Cr-Ti alloys that the

two stages described above are observed with soft x-radiation but only one stage is found with hard radiation. This supports the suggestion that the appearance of two different intermediate structures during aging is only a matter of degree in a continuously changing system. (Kelly and Nicholson[2] have reviewed the work of Bagaryatskii and Tyapkin and other work pertinent to the present investigation.)

The microstructure of greatest interest is the one which gives the maximum room temperature yield stress for any given aging temperature. This maximum occurs at a time when the magnetic coercivity and other properties[9] are at a maximum and when the transformation is still in the "side-band" stage. The "side-band" microstructure can be considered as two tetragonal structures with $c/a < 1$ and $c/a > 1$ where a is constant and c is a function of position. Thus a one dimensional lattice parameter fluctuation occurs. The basic assumption employed in the theory to be developed is that the tetragonality of the two structures is caused by elastic strains needed to maintain coherency of two structures that, if unattached, would be cubic. It has been shown that structures of all compositions in Cu-Ni-Fe alloys are cubic when quenched from above the miscibility gap[12] and they are cubic when overaging has caused a loss of coherency.[7] One of the strained structures has a cubic parameter that is too small to match with the other and consequently plates of this structure will be stressed in two dimensional tension in the coherent state. Likewise plates of the other structure will be stressed in compression. It has been suggested[13] that these coherency strains inhibit the transformation such that the composition maxima do not reach those given by the equilibrium diagram until coherency is lost.

The end effects introduce a complication in the stress analysis, but if it is assumed that the plates are long compared to their thickness, the end effects can be neglected. Moderate deflections at the ends of long plates cause only slight changes in the strain along the length of the plates. An electron microscope study of the structures which form during spinodal decomposition is in progress and it indicates that the plates in Cu-Ni-Fe alloys are indeed long compared to their width.

THE INTERNAL STRESSES

The method to be followed in calculating the yield stress is to determine the magnitudes of the internal stresses present in coherent lamellar microstructures and to resolve these stresses along the slip plane in order to relate them to the first large migration of dislocations enforced by a gradually increasing load. In the analysis, a square wave composition-distance curve will first be assumed. The resulting structure will then be as shown in Fig. 1. The subscripts 1 and 2 refer respectively to the properties of the structure with $c_1/a < 1$ and to the structure with $c_2/a > 1$. Let $\bar{a}$ represent the common non-equilibrium "a" parameter of the two tetragonal structures, and let a_{10} and a_{20} be the equilibrium cubic lattice parameters for structures having the most extreme compositions existing in the plates. These two values will tend to approach those of the equilibrium phases predicted by the phase diagram.

The lamellar plates are considered to be parallel to the x-y plane in the following derivation but the results are equally valid for plates lying parallel to either x-z or y-z planes. The x-y plane is taken to be parallel to (001). The cross-hatched plane of Fig. 1 represents a cut section through the lamella and the external forces F_{x1} and F_{x2}

replace the constraints which were present before the cut; λ is the wavelength of the composition fluctuation and f_1 and $f_2 = (1-f_1)$ are the volume fractions of the two structures. Because $c_1 < \bar{a}$ and $c_2 > \bar{a}$ the total displacement over many lamellae in the z direction will be small and therefore the assumption is made that $\sigma_{zz} = 0$ where σ_{zz} is the stress in the z direction. The effect of having σ_{zz} differ from zero is to raise the stresses in plates of one composition while it lowers the stresses in the plates of the other composition by a corresponding amount. The net effect eventually nearly cancels when the final calculations are made (cf. Eq. (18)).

From $\Sigma F_x = 0$ and Fig. 1 it can be seen that

$$\sigma_{xx1} L\lambda f_1 = -\sigma_{xx2} L\lambda f_2 . \tag{1}$$

(σ_{xx2} will have a negative sign showing compression because plus x is taken to be the positive direction of stress.) Because the structures are tetragonal and are not orthorhombic, $\sigma_{xx} = \sigma_{yy}$ in both structures. σ_{xx1} and σ_{xx2} are constants when a square wave composition-distance curve is assumed.

Equation (1) can also be obtained for a more general composition-distance wave form. For this case let σ_{xx1} vary across plates of composition 1 according to the expression.

$$\sigma_{xx1} = \sigma_{xx1}\Big|_{max} \sum_{\substack{1 \\ n\,odd}}^{n} A_{1n} \sin \frac{2\pi nz}{\lambda_1}, \quad (0 \leq z \leq \frac{\lambda_1}{2}) \tag{2}$$

where the maximum amplitude of $\sum_{1}^{n} A_{1n} \sin \frac{2\pi nz}{\lambda_1}$, for n odd, is restricted to unity. Therefore $\sigma_{xx1} \leq \sigma_{xx1}\Big|_{max}$ where $\sigma_{xx1}\Big|_{max}$ is a constant. Also in plates of composition 2

$$\sigma_{xx2} = \sigma_{xx2}\Big|_{max} \sum_{\substack{1 \\ n\ odd}}^{n} A_{2n} \sin \frac{2\pi nz}{\lambda_2}, \quad \left(\frac{\lambda_2}{2} \leq z \leq \lambda_2\right)$$

or

$$\sigma_{xx2} = -\sigma_{xx2}\Big|_{max} \sum_{\substack{1 \\ n\ odd}}^{n} A_{2n} \sin \frac{2\pi nz'}{\lambda_2}, \quad \left(0 \leq z' \leq \frac{\lambda_2}{2}\right) \qquad (3)$$

where $z' = z - \lambda_2/2$ and $|\sigma_{xx2}| \leq \sigma_{xx2}\big|_{max}$. $\sigma_{xx2}\big|_{max}$ is a positive constant and σ_{xx2} is always a compressive stress, i.e., $\sigma_{xx2} < 0$. λ_1 and λ_2 are related to the modulation wavelength by

$$\frac{\lambda_1}{2} + \frac{\lambda_2}{2} = \lambda ,$$

and the volume fractions f_1 and f_2 are related to λ_1 and λ_2 by

$$\frac{f_1}{f_2} = \frac{\lambda_1}{\lambda_2} . \qquad (4)$$

Again, $\Sigma F_x = 0$ and

$$L \int_0^{\frac{\lambda_1}{2}} \sigma_{xx1}\Big|_{max} \sum_{\substack{1 \\ n\ odd}}^{n} A_{1n} \sin \frac{2\pi nz}{\lambda_1}\, dz = -L \int_0^{\frac{\lambda_2}{2}} -\sigma_{xx2}\Big|_{max} \sum_{\substack{1 \\ n\ odd}}^{n} A_{2n} \sin \frac{2\pi nz'}{\lambda_2}\, dz . \qquad (5)$$

On integrating both sides of the equation between the given limits

$$\sigma_{xx1}\Big|_{max} \frac{\lambda_1}{2\pi} \left\{ \sum_{\substack{1 \\ n\ odd}}^{n} \left(\frac{A_{1n}}{n} \cos \pi n - \frac{A_{1n}}{n} \right) \right\} = \sigma_{xx2}\Big|_{max} \frac{\lambda_2}{2\pi} \left\{ \sum_{\substack{1 \\ n\ odd}}^{n} \left(\frac{A_{2n}}{n} \cos \pi n - \frac{A_{2n}}{n} \right) \right\} .$$

If the two wave shapes are similar such that $A_{1n} = A_{2n}$, then

$$\left(\sigma_{xx1}\Big|_{max}\right) \frac{\lambda_1}{2\pi} = \left(\sigma_{xx2}\Big|_{max}\right) \frac{\lambda_2}{2\pi} \quad ,$$

and using Eq. (4)

$$\sigma_{xx1}\Big|_{max} f_1 = \sigma_{xx2}\Big|_{max} f_2. \tag{6}$$

The maximum value of σ_{xx1} is $\sigma_{xx1}\Big|_{max}$ (cf. Eq. (2)), and the extreme value of $|\sigma_{xx2}|$ is $\sigma_{xx2}\Big|_{max}$, i.e., $\sigma_{xx2} = -\sigma_{xx2}\Big|_{max}$ (cf. Eq. (3)), then again

$$\sigma_{xx1} f_1 = -\sigma_{xx2} f_2 \tag{7}$$

for the conditions of identical wave form. This is identical to Eq. (1) when L and λ are cancelled in the earlier equation. Hereafter the subscripts denoting maximum stress will be dropped, and σ_{xx1} and σ_{xx2} will be used to indicate maximum values of these two stresses. Only stress maxima need be considered in the following analysis because dislocations will encounter the greatest barriers where the stresses are largest.

The maximum stresses can be determined, when the corresponding strains are known, from the relationships of Eq. (8) for anisotropic cubic cyrstals.

$$\left.\begin{aligned}
e_{xx} &= S_{11}\sigma_{xx} + S_{12}\sigma_{yy} + S_{12}\sigma_{zz} \\
e_{yy} &= S_{12}\sigma_{xx} + S_{11}\sigma_{yy} + S_{12}\sigma_{zz} \\
e_{zz} &= S_{12}\sigma_{xx} + S_{12}\sigma_{yy} + S_{11}\sigma_{zz} \\
e_{yz} &= S_{44}\sigma_{yz} \\
e_{zx} &= S_{44}\sigma_{zx} \\
e_{xy} &= S_{44}\sigma_{xy}
\end{aligned}\right\} \tag{8}$$

The first subscript of the stresses and strains in Eq. (8) refers to the normal of the plane over which the stresses act while the second gives the direction of their action. S_{11}, S_{12}, and S_{44} are the elastic compliances for cubic crystals. As previously mentioned, when the lamellar plates lie in the x-y plane, $\sigma_{xx} = \sigma_{yy}$ and $\sigma_{zz} = 0$. In addition, $\sigma_{xy} = 0$ because the two structures are tetragonal and the x-y plane is taken perpendicular to the four-fold axis of rotation. σ_{yz} and σ_{xz} are not zero, but for plates that are long compared to their thickness, these shear stresses are small. σ_{yz} and σ_{xz} will be greatest at the boundary between structures 1 and 2 where they are related to $\sigma_{xx}|_{max}$ by the ratio of λ/L. For thin plates $\lambda << L$ and λ/L is small so that σ_{yz} and σ_{xz} can be neglected. Therefore

$$\left.\begin{aligned} e_{xx} &= (S_{11} + S_{12})\ \sigma_{xx} \\ e_{yy} &= (S_{11} + S_{12})\ \sigma_{xx} \\ e_{zz} &= 2S_{12}\ \sigma_{xx} \end{aligned}\right\}, \tag{9}$$

and

$$\sigma_{xx} = \frac{e_{xx}}{S_{11} + S_{12}}. \tag{10}$$

Applying Eq. (1) or (7),

$$\frac{e_{xx1}\ f_1}{(S_{11} + S_{12})_1} = - \frac{e_{xx2}\ f_2}{(S_{11} + S_{12})_2} \tag{11}$$

where the subscripts outside the parentheses refer to the data for structure one and two respectively. By substituting $e_{xx} = \dfrac{\bar{a} - a_o}{a_o}$ into Eq. (11) and solving for $\bar{a}$,

$$\bar{a} = \frac{a_{10}a_{20}\{f_1(S_{11} + S_{12})_2 + f_2(S_{11} + S_{12})_1\}}{a_{20}f_1(S_{11} + S_{12})_2 + a_{10}f_2(S_{11} + S_{12})_1} . \qquad (12)$$

Equation (10) can be rewritten

$$\sigma_{xx} = \frac{\bar{a} - a_o}{(S_{11} + S_{12})a_o} \qquad (13)$$

so that when the elastic compliances and cubic lattice parameters are known, Eq. (13) can be used to evaluate the principle stresses in each plate.

From Eqs. (9) and (10),

$$e_{zz} = \frac{2S_{12}e_{xx}}{S_{11} + S_{12}}$$

and $\frac{c - a_o}{a_o} = \frac{2S_{12}}{S_{11} + S_{12}} \frac{(\bar{a} - a_o)}{a_o}$, therefore

$$c = a_o + \frac{2S_{12}}{S_{11} + S_{12}} (\bar{a} - a_o) \qquad (14)$$

or, if $\bar{a}$ and the $c/\bar{a}$ ratio are known for each structure, then the cubic parameters can be obtained by rearranging Eq. (14) and

$$a_o = \frac{1}{S_{11} - S_{12}} \{(S_{11} + S_{12})c - 2S_{12}\bar{a}\} . \qquad (15)$$

THE EFFECT OF INTERNAL AND APPLIED STRESSES ON DISLOCATION MOTION

In order to find the effects of σ_{xx1} and σ_{xx2} on dislocation motion, shear components of these stresses on the slip plane and in the slip direction must be found. For FCC crystals the slip plane is {111} and the slip direction is ⟨110⟩ . Resolution of these stresses can be done with the aid of a stress tensor. On using the tensor method, the stress

in the ν direction, when the normal to the slip plane is given by μ, is

$$\sigma_{\mu\nu} = \sum_{ij} \sigma_{ij} \ell_{i\mu} \ell_{j\nu} \tag{16}$$

$$i = x,y,z$$
$$j = x,y,z$$

where $\ell_{i\mu}$ and $\ell_{j\nu}$ are direction cosines between the given lines. Letting μ be normal to the (111) plane and ν be in $[10\bar{1}]$, then, when the lamellar plates lie in the x-y plane,

$$\sigma_{(111)[10\bar{1}]} = \sigma_{xx} \ell_{[100][111]} \ell_{[100][10\bar{1}]} + \sigma_{xx} \ell_{[010][111]} \ell_{[010][10\bar{1}]}$$

where

$$\ell_{[100][111]} = \frac{1}{\sqrt{3}}, \quad \ell_{[100][10\bar{1}]} = \frac{1}{\sqrt{2}}, \quad \ell_{[010][111]} = \frac{1}{\sqrt{3}},$$

and $\ell_{[010][10\bar{1}]} = 0$. Therefore $\sigma_{(111)[10\bar{1}]} = \frac{\sigma_{xx}}{\sqrt{6}}$.

Likewise, $\sigma_{(111)[01\bar{1}]} = \frac{\sigma_{xx}}{\sqrt{6}}$ but $\sigma_{(111)[\bar{1}10]} = 0$.

These stresses are pure shear components because ν is normal to μ.

Consider a dislocation in the (111) plane with Burger's vector $\frac{a}{2}[10\bar{1}]$. For plates which are parallel to (001), (i.e., parallel to the x-y plane), we have seen that $\sigma_{(111)[10\bar{1}]} = \frac{\sigma_{xx}}{\sqrt{6}}$. An adjoining set of plates will be parallel to either (010) or (100). For plates parallel to (010), $\sigma_{xx} = \sigma_{zz}$ and $\sigma_{yy} = 0$ so that the shear stress acting on the above dislocation while it is in these plates is

$$\sigma_{(111)[10\bar{1}]} = \sigma_{xx} \ell_{x\mu} \ell_{x\nu} + \sigma_{zz} \ell_{z\mu} \ell_{z\nu}$$

$$= \sigma_{xx} \frac{1}{\sqrt{3}} \frac{1}{\sqrt{2}} + \sigma_{xx} \frac{1}{\sqrt{3}} \left(-\frac{1}{\sqrt{2}}\right) = 0.$$

For plates parallel to (100), $\sigma_{xx} = 0$, and $\sigma_{yy} = \sigma_{zz}$ so that

$$\sigma_{(111)[10\bar{1}]} = \sigma_{yy}\ell_{y\mu}\ell_{y\nu} + \sigma_{zz}\ell_{z\mu}\ell_{z\nu}$$

$$= \sigma_{yy}\frac{1}{\sqrt{3}}(0) + \sigma_{yy}\frac{1}{\sqrt{3}}\left(-\frac{1}{\sqrt{2}}\right) = -\frac{\sigma_{yy}}{\sqrt{6}} .$$

The magnitude of σ_{yy} for plates parallel to (100) is the same as the magnitude of σ_{xx} for plates parallel to (001).

Because a dislocation will interact with these three plate orientations with equal probability, one-third of a unit length of dislocation will experience an accelerating stress from plates parallel to (001) when $\sigma_{xx} > 0$, one-third will experience zero stress from plates parallel to (010), and the remainder will experience a retarding stress from plates parallel to (100) when $\sigma_{yy} > 0$. The portion of the dislocation which is accelerated will move until it encounters an adjacent tetragonal plate that is loaded in compression so that $\sigma_{xx} < 0$ and $\sigma_{(111)[10\bar{1}]} = -\frac{|\sigma_{xx}|}{\sqrt{6}}$, which is now a retarding stress. Consequently, the dislocation will be retarded along one-third of its length by plates which are in compression, experience zero stress along one-third of its length, and be retarded along the remaining third by plates that are loaded in tension. Dislocations in other slip systems will encounter identical conditions. The maximum retarding force on a unit dislocation will be,

$$F = \frac{1}{3}|\tau_1|b + \frac{1}{3}|\tau_2|b + 0 \qquad (17)$$

where $|\tau_1|$ is the absolute value of the resolved shear stress acting on dislocations with Burgers vector b from plates which are in tension (for plate orientations where $\tau_1 \neq 0$), and $|\tau_2|$ is the absolute value of the

resolved shear stress from plates which are in compression (for plate orientations where $\tau_2 \neq 0$). Now $|\tau_1| = \frac{\sigma_{xx1}}{\sqrt{6}}$ and $|\tau_2| = -\frac{\sigma_{xx2}}{\sqrt{6}}$ so that $F = \frac{1}{3}\frac{1}{\sqrt{6}}(\sigma_{xx1} - \sigma_{xx2})b$ where the negative sign appears before σ_{xx2} because of its compressive nature. The applied stress which must overcome this force if dislocations are to move is $\tau_{app} = \frac{F}{b}$ or

$$\tau_{app} = \frac{1}{3\sqrt{6}}(\sigma_{xx1} - \sigma_{xx2}) . \tag{18}$$

However, when $\tau_{app} > |\tau_2|$, which can happen when f_2 is large and structure 2 contains a small strain, then Eq. (18) no longer governs the stress for the first dislocation motion. In this case the applied stress will cause the dislocation segment inhibited by τ_2 to move through structure 2 until it reaches structure 1 where it will be accelerated. Thus only one-third of the unit length of dislocation line will be retarded while the other two segments will have either zero shear stress or an accelerating stress. The net effect is that plastic flow can easily take place. The applied stress τ_{app} needed to start this chain of events is

$$\tau_{app} = |\tau_2| = -\frac{\sigma_{xx2}}{\sqrt{6}} . \tag{19}$$

CRITICAL VOLUME FRACTIONS

The shear stresses τ_1 and τ_2 are dependent on the volume fractions of the two structures present. By equating the applied stress to $|\tau_2|$ in Eq. (18), a solution for the critical volume fraction where Eq. (18) will break down can be obtained. Therefore,

$$|\tau_2| = -\frac{\sigma_{xx2}}{\sqrt{6}} = \frac{1}{3\sqrt{6}}(\sigma_{xx1} - \sigma_{xx2}) \tag{20}$$

and

$$2\sigma_{xx2} = -\sigma_{xx1}.$$

Using Eqs. (1) or (7),

$$\frac{\sigma_{xx1}}{\sigma_{xx2}} = -\frac{f_2}{f_1} = -\frac{f_2}{1-f_2} = -2.$$

Solving for f_2 thus yields $f_2 = \frac{2}{3}$ and $f_1 = \frac{1}{3}$. Similar equations can be derived for the case when $\tau_{app} = |\tau_1|$. The solution for this case will give $f_1 = \frac{2}{3}$ and $f_2 = \frac{1}{3}$. Thus equation (18) is good for $\frac{1}{3} \leq f_1 \leq \frac{2}{3}$.

SIMPLIFICATIONS WHEN $(S_{11} + S_{12})_1 = (S_{11} + S_{12})_2$

If Eq. (18) is valid, and $(S_{11} + S_{12})_1 = (S_{11} + S_{12})_2$, then Eqs. (12), (13), and (18) can be combined to give a simplified equation for the applied yield stress of alloys which have volume fractions between the critical limits. Thus

$$\bar{a} = \frac{a_{10}a_{20}(f_1 + f_2)}{a_{20}f_1 + a_{10}f_2}, \tag{21}$$

and

$$\sigma_{xx_1} = \frac{\bar{a} - a_{10}}{(S_{11} + S_{12})a_{10}} = \frac{1}{(S_{11} + S_{12})}\left\{\frac{a_{20}}{a_{20}f_1 + a_{10}f_2} - 1\right\},$$

and

$$\sigma_{xx_2} = \frac{1}{(S_{11} + S_{12})}\left\{\frac{a_{10}}{a_{20}f_1 + a_{10}f_2} - 1\right\}.$$

Therefore, from Eq. (18),

$$\tau_{app} = \frac{1}{3\sqrt{6}} \frac{1}{S_{11} + S_{12}} \left\{ \frac{a_{20} - a_{10}}{a_{20} f_1 + a_{10} f_2} \right\}$$

but because $a_{10} \approx \bar{a} \approx a_{20}$,

$$\tau_{app} \approx \frac{1}{3\sqrt{6}} \frac{1}{(S_{11} + S_{12})} \left(\frac{\Delta a_o}{\bar{a}} \right) . \qquad (22)$$

Thus the yield stress is directly proportional to the difference in lattice parameters of the two extreme compositions when Eq. (18) is valid. Usually the elastic moduli do not differ widely in metal systems and direct proportionality can often be expected.

When τ_{app} is given by Eq. (19), a general relationship between yield stress and volume fraction can be obtained if it is again assumed that the sums of the elastic moduli are the same for both structures. From Eqs. (13) and (19),

$$\tau_{app} = |\tau_2| = - \frac{\sigma_{xx2}}{\sqrt{6}} = - \frac{1}{\sqrt{6}} \frac{(\bar{a} - a_{20})}{(S_{11} + S_{12}) a_{20}} .$$

When $(S_{11} + S_{12})_1 = (S_{11} + S_{12})_2$, $\bar{a}$ is given by Eq. (21), and

$$\tau_{app} = - \frac{1}{\sqrt{6}} \frac{1}{(S_{11} + S_{12})} \left\{ \frac{a_{10}}{a_{20} f_1 + a_{10} f_2} - 1 \right\} ,$$

and on rearranging

$$\tau_{app} = \frac{1}{\sqrt{6}} \frac{1}{(S_{11} + S_{12})} \frac{1}{1 + \frac{a_{10}}{\Delta a_o f_1}} ,$$

but

$$\frac{a_{10}}{\Delta a_o f_1} >> 1 ,$$

then

$$\tau_{app} = \frac{1}{\sqrt{6}} \frac{f_1}{(S_{11} + S_{12})} \left(\frac{\Delta a_o}{a_{10}}\right) . \qquad (23)$$

Equation (23) is valid for $f_1 < \frac{1}{3}$. Thus the yield stress is directly proportional to the difference in cubic lattice parameters and the volume fraction of structure 1 for the above conditions. For $f_1 << \frac{1}{3}$, Eq. (23) will not be reliable because of the loss of uniform strain fields for small volume fractions of precipitate. This is the case for most precipitation hardening systems. It is clear from this discussion that Eq. (22) gives an estimate of the maximum attainable yield stress for any precipitation hardening system having plate-like precipitates where coherency strains are controlling because the yield stress does not increase after the critical volume fraction is exceeded.

SUMMARY AND CONCLUSIONS

For alloys that have $(S_{11} + S_{12})_1 = (S_{11} + S_{12})_2$, Eqs. (22) and (23) show that the yield stress is directly proportional to the difference in cubic lattice parameters. When $(S_{11} + S_{12}) \neq (S_{11} + S_{12})_2$, the results of Eqs. (12), (13), and (18) can be combined to give the yield stress if the elastic constants, volume fractions, and cubic lattice parameter for the extreme compositions are known. Numerical calculations[14] using Eqs. (12), (13), and (18) have shown that the yield stress is proportional to the difference in cubic lattice parameters even when $(S_{11} + S_{12})_1 \neq (S_{11} + S_{12})_2$ for a given alloy.

The equations derived above show four significant points:

1. The yield stress is directly proportional to the difference in the cubic lattice parameters of the two chemically different lamellae forming the lamellar microstructure.

2. For alloys containing volume fractions of one kind of lamellae below the critical value of $\frac{1}{3}$, the yield stress is directly proportional to this volume fraction.

3. For alloys containing volume fractions between critical values $\left(\frac{1}{3} \text{ to } \frac{2}{3}\right)$, the yield stress is independent of volume fraction.

4. The yield stress is independent of λ, the modulated structure wavelength, which means the yield stress is independent of the interlamellar spacing or particle size present.

Points 1, 3, and 4 have been experimentally verified for alloys of Cu-Ni-Fe with volume fractions between the critical limits. These results will be found in a subsequent report.[14]

ACKNOWLEDGEMENTS

The author wishes to thank Professor E. R. Parker for helpful discussions. This work is included in the author's Ph.D. Thesis and was financially supported by the United States Atomic Energy Commission.

FIGURE CAPTIONS

Fig. 1 Model used to determine the stresses in coherent lamellar plates. Front surface (shaded) represents a plane cut through the lamella and the forces F_{x1} and F_{x2} represent replacements for the constraints which were removed by cutting.

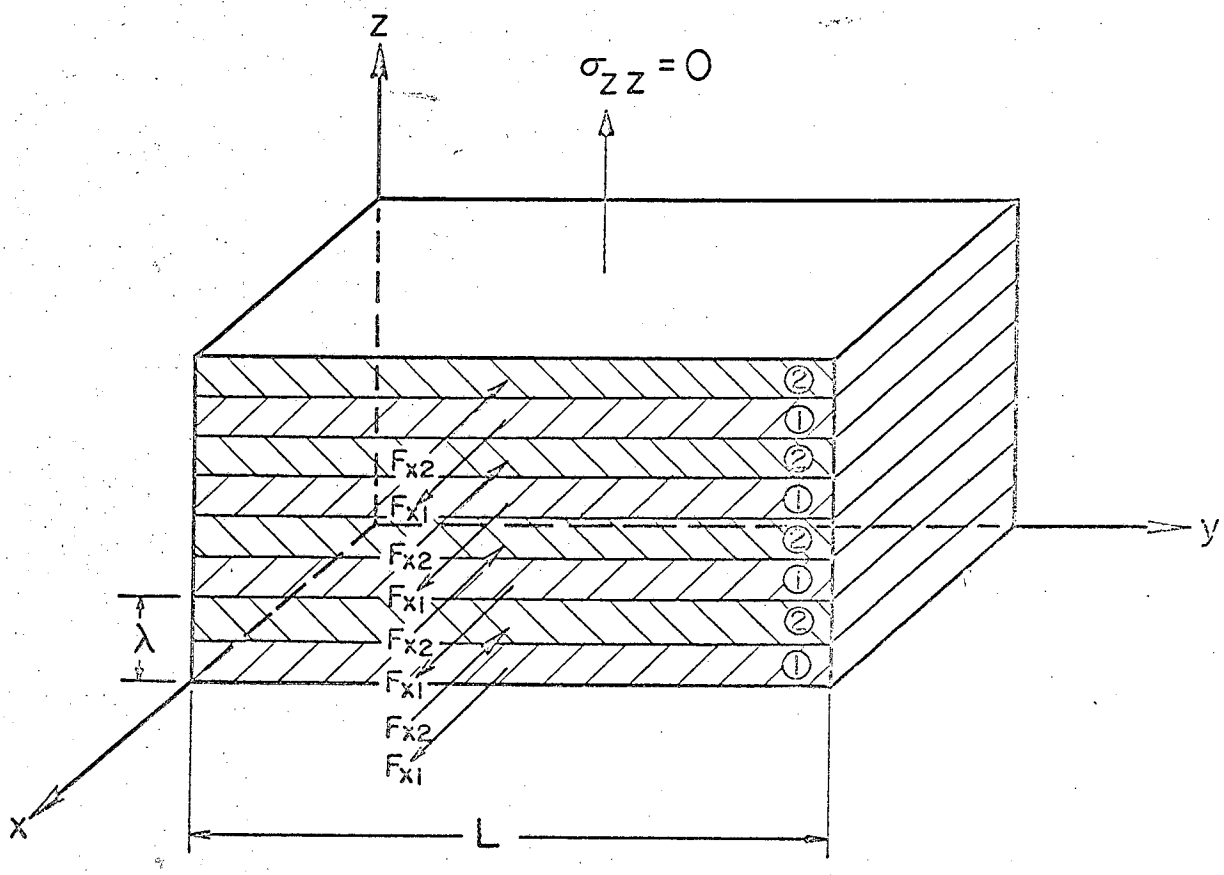

MUB-9674

Fig. 1

This report was prepared as an account of Government sponsored work. Neither the United States, nor the Commission, nor any person acting on behalf of the Commission:

A. Makes any warranty or representation, expressed or implied, with respect to the accuracy, completeness, or usefulness of the information contained in this report, or that the use of any information, apparatus, method, or process disclosed in this report may not infringe privately owned rights; or

B. Assumes any liabilities with respect to the use of, or for damages resulting from the use of any information, apparatus, method, or process disclosed in this report.

As used in the above, "person acting on behalf of the Commission" includes any employee or contractor of the Commission, or employee of such contractor, to the extent that such employee or contractor of the Commission, or employee of such contractor prepares, disseminates, or provides access to, any information pursuant to his employment or contract with the Commission, or his employment with such contractor.